Sustainable Production through Advanced Manufacturing, Intelligent Automation and Work Integrated Learning, J. Andersson et al. (Eds.)

doi:10.3233/ATDE240172

Anomaly Detection in Optical Monitoring of Laser Beam Welding

Morgan NILSEN[a,1]
[a] *University West, Department of Engineering Sciences, Trollhättan, Sweden*

ORCiD ID: Morgan Nilsen https://orcid.org/0000-0002-8771-7404

Abstract. Robotized laser beam welding is one important process in manufacturing, offering efficient welding while minimizing the heat input. Nonetheless, this method is sensitive to various deviations, including fixture problems, heat-induced distortions, and inaccuracies in tool handling. Such deviations can lead to significant defects like lack of fusion, particularly when welding square butt joints without gaps. Detecting these defects through visual inspection or non-destructive methods is challenging. To address this, real-time monitoring and automatic intervention are necessary. One effective sensor for monitoring laser beam welding is the photodiode, which captures optical emissions from the process. Research has demonstrated correlations between these emissions and process stability. Photodiodes are cost-effective and easily integrated into welding tools, making them ideal for industrial applications. However, the challenge lies in analyzing the output signals and defining thresholds for identifying deviations from normal conditions. Thus, there's a need for an automated method to set threshold values based on measured data. Machine learning offers a solution, particularly through supervised, unsupervised, or semi-supervised methods. Supervised machine learning requires labeled data, involving time-consuming experiments with nominal and deviating cases, making it less feasible for industrial setups. This paper suggests using unsupervised learning for anomaly detection, relying solely on data from nominal welding cases for model training. In this approach, a model is trained using photodiode data from a single nominal weld case and subsequently tested on data collected during experiments involving laser beam offsets during welding. The results demonstrate the promise of this method for monitoring closed square butt-joint laser beam welding, even with limited training data from nominal cases.

Keywords. Laser beam welding, anomaly detection, machine learning, photodiodes

1. Introduction

Laser beam welding (LBW) enables narrow and deep welds with a limited heat-affected zone (HAZ), which in turn reduces the thermal distortion of the welded components. One disadvantage of using LBW is its sensitivity to deviations in positioning the laser beam with respect to the joint position. Even a small offset from the nominal path, hereafter called beam offset, could result in lack of sidewall fusion in the welded seam. Inaccuracies in fixturing, tolerances in the robot motion, distortion of the welded components, etc. yield deviations from the nominal weld path. Seam tracking, or joint tracking, is one solution to this issue and is traditionally accomplished using a camera

[1] Corresponding Author: Morgan Nilsen, morgan.nilsen@hv.se.

and some kind of structured light. Several commercial systems that use this method are available, e.g.; (1). However, this solution requires a rather big investment, since it consists of both a sensor solution and hardware to move the laser beam. In some situations, there is a need for a simpler go/no-go system that informs the operator if the welding was successful or not. One relatively simple and cost-effective solution is to use photodiodes to monitor the spectral emissions from the process. The main challenge with those systems is however the analysis of the sensor signals since it is an indirect measurement of weld position, and it is not obvious how the sensor signals are related to the process deviations. One promising method of analyzing the sensor signals is to use machine learning (ML) to classify the process state based on the sensor signals. Previous work on analyzing photodiode signals by ML uses supervised learning. This requires data to be produced by several welding cases that are not nominal since data of all classes needs to be acquired. This is time-consuming and might not be possible in an industrial setup. The approach presented in this paper instead uses unsupervised learning where only data from a nominal test case is needed for training.

Numerous studies have addressed the endeavor of establishing correlations between LBW processes and the spectral emissions originating from the processes, utilizing photodiode-based sensing techniques. Eriksson et al. (2) (3) conducted an investigation into photodiode-based monitoring employing a commercial system manufactured by Precitec. Their research unveiled several significant findings. Firstly, their work demonstrated the potent utility of high-speed imaging as a valuable tool for assessing the capacity of photodiode systems to discern specific welding defects. Concurrently, their study clarified an inherent limitation: the high-frequency dynamics of the plasma plume overshadow other pertinent process dynamics, thereby diminishing the effectiveness of photodiode-based monitoring. Moreover, Eriksson et al. highlighted the viability of monitoring the reflected laser light as a valuable metric for assessing weld quality, especially within the context of pulsed LBW. Olsson et al. (4) presented a comprehensive analysis of photodiode-monitored LBW, specifically for zinc-coated steel. They tackled the challenge of interpreting raw photodiode data and proposed a novel approach involving the analysis of data within a three-dimensional cloud. Their investigation indicated that during unstable welding conditions, the variance in reflected laser light intensifies. Kawahito et al. (5) contributed to the field by developing a feedback control system for full penetration welding. Their experimental endeavors, welding thin titanium samples, showcased the feasibility of maintaining stable weld penetration by regulating laser power based on the heat radiation intensity measured by a photodiode. Furthermore, Sibillano et al. (6) monitored the plasma plume dynamics during CO2 LBW using a single silicon photodiode. They analyzed fluctuations within the plasma plume, presuming direct correlations with melt pool and keyhole instabilities. Application of a discrete wavelet transform (DWT) on the photodiode signal unveiled valuable insights into LBW process changes arising from laser power variations and alterations in shielding gas flow. Elefante et al. (7) presented a monitoring system encompassing a photodiode to examine spectral emissions from the plasma plume during LBW, with a specific focus on beam offsets. Continuous wavelet transform analysis of the photodiode signal unveiled a correlation between the signal and beam offset variations.

More recently, several researchers have applied machine learning algorithms to find correlations between photodiode signals and process deviations in LBW. Lee et al. (8) evaluated different machine learning algorithms (support vector machine, fully connected neural network, and convolutional neural network), to classify penetration depth in overlap LBW of Al/Cu joints for electric vehicle batteries. It was shown that the

penetration depth classification algorithms, verified by an optical coherence tomography system, all could achieve more than 90 % accuracy. Chianese et al. (9) studied if photodiode signals together with supervised machine learning could classify defects during remote laser welding of thin foils. Seven supervised machine learning algorithms were evaluated; k-nearest neighbors, decision tree, random forest, Naïve–Bayes, support vector machine, discriminant analysis, and discrete wavelet transform combined with the neural network. It was shown that an accuracy of up to 97 % could be achieved for variations in weld penetration and gaps between parts. Kang et al. (8) presented a study where penetration depth was predicted using a CNN model trained from weld pool images and photodiode signals. Promising results were shown for penetration depth prediction in LBW of Al/Cu overlap joints. Zhang et al. (10) presented a multi-sensor system comprising auxiliary illumination, a visual sensor system, a UVV band visual sensor system, a spectrometer, and two photodiodes. Based on features of the LBW process, a convolutional neural network was developed to detect welding defects.

Even though previous research shows promising results, no studies show a photodiode monitoring system for detecting beam offsets using unsupervised ML. Previously presented methods require data to be acquired for several non-nominal cases, that is experiments for provoking defects needs to be developed and executed, while the study presented in this work can be based on nominal production data.

2. Experimental Setup

The laser source utilized in this study was an IPG Ytterbium Fiber Laser (YLR-6000-S, 6 kW) emitting radiation at a wavelength of 1070 nm. The LBW tool employed in the experimental setup was supplied by Permanova Lasersystem AB. The configuration involved a 160 mm focal length collimator, a 300 mm focal length focusing lens, and a 600 μm optical fiber, producing a laser beam spot with a diameter of 1.12 mm and a Rayleigh length of 13.7 mm. The laser beam was focused onto the workpiece surface with a laser power setting of 2750 W, facilitating keyhole welding. The robot's traverse speed was maintained at 9.6 mm/s. Both the laser power and robot speed were empirically optimized to yield visually satisfactory weld seams.

The LBW tool manipulation was conducted using an ABB IRB4400 industrial robot. The positional data of the tool center point, where the laser spot made contact with the workpiece, was continuously acquired from the robot control system. This positional data was synchronized with the photodiode measurements to establish correlations between signal variations and the laser spot's position on the workpiece.

Welding was executed without the utilization of filler material, employing 4 mm thick stainless steel (ss316) plates configured in a closed-square-butt joint with no gap. These plates were preliminarily tack-welded at intervals of approximately 50 mm and secured in a fixture to mitigate heat-induced distortions and gap width alterations during welding. Argon gas was employed as the shielding gas, with a flow rate of 32 l/min introduced from the top side through a 10 mm diameter tube and on the root side through a gas channel integrated within the fixture. Additionally, argon gas was supplied in front of the focusing lens of the LBW tool to safeguard it against spatter generated by the vapor plume.

A monitoring system featuring two photodiodes with a specified spectral range was developed to observe the optical emissions from the vapour plume during the LBW process. The photodiodes were coaxially integrated into the LBW tool as shown in

Figure 1. Two fiber-coupled photodetectors were used, one monitoring wavelengths ranging from 340-600 nm (hereafter referred to as the P-sensor), and one monitoring the wavelength around 1070 nm (hereafter referred to as the R-sensor). Optical filters were used to limit the spectral ranges of the photodetectors. The P-sensor intended to capture the spectral emissions from the vapour plume while the R-sensor intended to capture reflected laser light. Both the P-sensor and the R-sensor signals were sampled synchronously at a sample rate of 100 kHz. Data was captured and stored using a LabView application implemented on a PC.

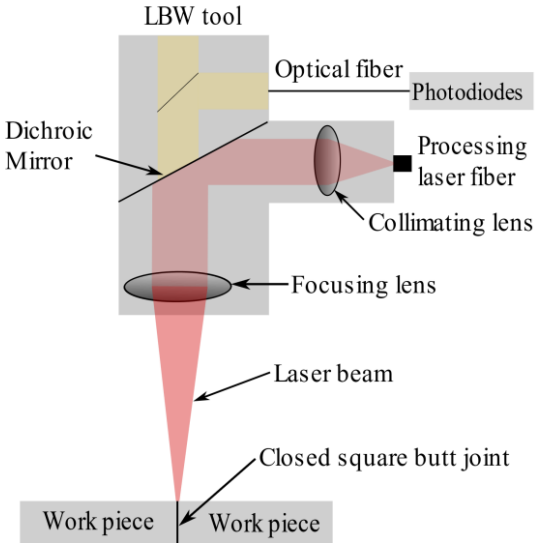

Figure 1. LBW tool and integration of photodiodes.

To evaluate the monitoring system's performance, two distinct test cases were executed. First, a reference weld, involving welding on closed-square-butt joints without any beam offset (hereafter referred to as TC1). The second test case addressed welding with beam offsets from the joint. Welding was initiated without a beam offset and then shifted 1.2 mm away from the joint, see upper graph in **Figure 2**. It was then followed by a return to the joint, repeated four times, see lower graph in **Figure 2**, This was conducted to assess the monitoring system's ability to detect beam offset conditions and is hereafter referred to as TC2.

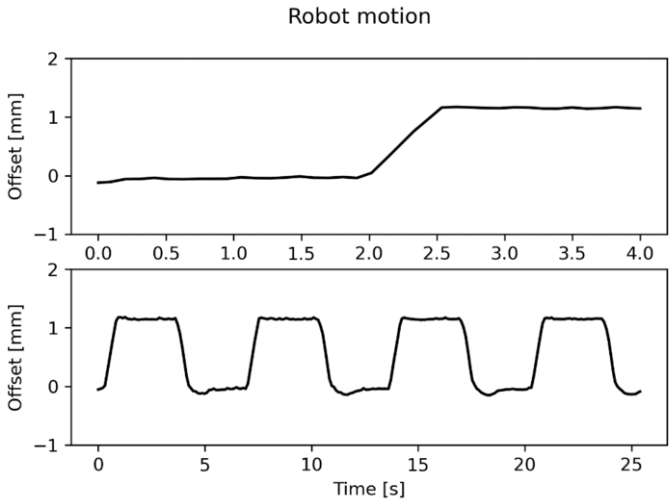

Figure 2. Robot motion for the second test case (TC2).

3. Algorithm

To find correlations between the photodiode signals and the beam offsets, One-Class Support Vector Machine (One-Class SVM) (11) was utilized for training models based on data from the nominal test case (TC1).

In essence, the objective of One-Class SVM revolves around constructing an approximate boundary that encapsulates the contour of the initial observations' (nominal reference welding data) distribution, depicted within a multidimensional embedding space. Subsequently, if subsequent observations fall within this boundary-defined subspace, they are regarded as originating from the same population as the initial observations. Conversely, if these observations lie beyond the established boundary, it is inferred that they deviate from the norm, and their abnormality can be ascertained with a certain degree of confidence. Details of the theoretical background of One-Class SVM can be found in (11).

4. Results and Discussion

Figure 3 shows the unfiltered data obtained from the P- and R-sensor during TC1 (nominal weld case). The startup sequence, before a stable process has been established, gave peaks in the sensor data that needed to be removed before it was used for training. Data used for training shall only represent stable welding conditions. Hence data from the startup and shutdown sequence was removed before it was used for training. **Figure 4** shows the unfiltered sensor data from the P- and R-sensor during TC2 (welding with beam offsets). The signal from the R-sensor shows slightly more variance while the signal from the P-sensor shows larger variance that could indicate correlations with the beam offset. It is however not obvious, by visually inspecting the signal values, if a strong correlation between sensor values and beams offset exists. **Figure 5** shows the filtered sensor values during a nominal welding case. Here a moving average filter of

500 samples has been applied and it reveals a relatively stable signal value of 0.1 for the P-sensor and 0.6 for the R-sensor. Compared with the filtered sensors values shown in **Figure 6** (using the same filter), with data from TC2, one can conclude that beam offsets seem to affect the signals both from the R- and P-sensor. The R-sensor signal shows small variations compared to the nominal test case and the P-sensor signal shows rather distinct variations that by visual inspection could be correlated to the beam offsets. It is however not obvious how to set the threshold for the signals, which motivates the data driven, model-based approach suggested in this paper.

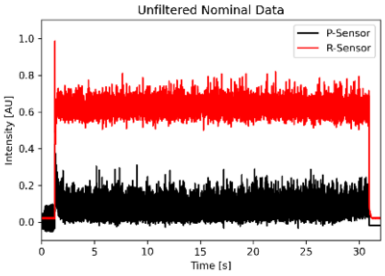

Figure 3. Raw unfiltered sensor data captured during the reference weld.

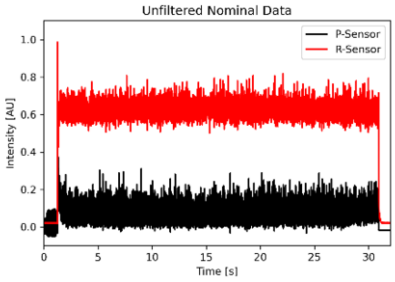

Figure 4. Raw unfiltered sensor data captured during the test case with beam offsets.

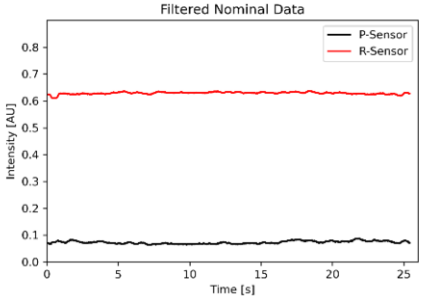

Figure 5. Filtered sensor data captured during the reference weld.

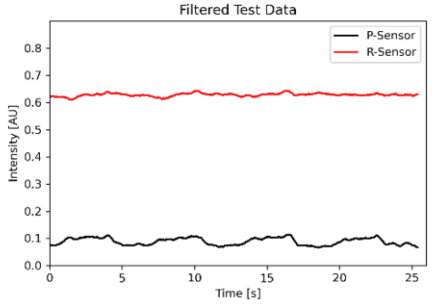

Figure 6. Filtered sensor data captured during the test case with beam offsets.

The histogram in **Figure 7** further confirms the hypothesis that the P-sensor could be closely correlated with the beam offsets. Two distinct peaks can be found, and it is reasonable to assume that those are connected to the two welding situations, welding in the joint and welding with a beam offset.

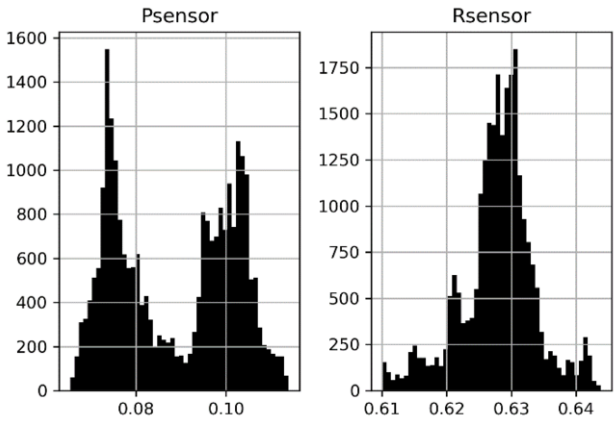

Figure 7. Histogram for the sensor data. The left plot shows the P-sensor and right plot shows the R-sensor.

To compare the influence of the different sensor signals, three different models were trained on data from TC1 and evaluated on TC2. The first model was trained on data from both the P- and the R-sensor, the second model was trained on data only from the P-sensor and the third model was trained on data only from the R-sensor. The labels used to evaluate the accuracy of each model were obtained from the robot motion. Positions more than 0.8 mm away from the joint were marked as having an *offset* and positions less or equal to 0.8 mm away from the joint were marked as having *no offset*. The accuracy of each model was then calculated by comparing the prediction values to the labels. The accuracy was calculated by dividing the number of correct predictions to the total number of predictions. **Table 1** shows the results from evaluating the three models on the test data from TC2. Using both the P- and R-sensor and only the P-sensor gave the same accuracy (86 %), however, only using the R-sensor gave significantly lower accuracy (56 %). This corresponds well to the previous observations indicating that the signal from the P-sensor seemed to be much more correlated to the beam offsets than the signal from the R-sensor.

Table 1. Accuracy of the predictions made for the three different models.

P- and R-sensor	P-sensor	R-sensor
86 %	86 %	56 %

Figure 8 shows plots from running the three different models on the test data (TC2). In the three upper plots, the red curve shows the predictions from the model and the black curve shows the labels (true values) based on calculations from the robot path. The fourth plot shows the robot motion for reference. Even though the models using both the P- and R-sensor and only the P-sensor gave the same accuracy, it is clear from the plots that the model using both the P- and the R-sensor gave more stable predictions. Using both the P- and R-sensor gave slightly more delay in detecting the beam offset. However, once the beam offset had been detected the predictions are consistent with the beam offsets. Using only the P-sensor gave slightly faster response to beam offsets. However, predictions are not consistent during sections with beam offsets. Using only the R-sensor

did not give good results, numerous misclassifications are visible which explains the inadequate accuracy of 56 %. It can be concluded that even if the model using both the P- and R-sensor and the model only using the P-sensor gave the same accuracy, the model using both sensors is preferred since in practice it gives more stable predictions. Once the robot has moved too far away from joint, this model could correctly predict this beam offset and did so until the robot had moved back to the join position.

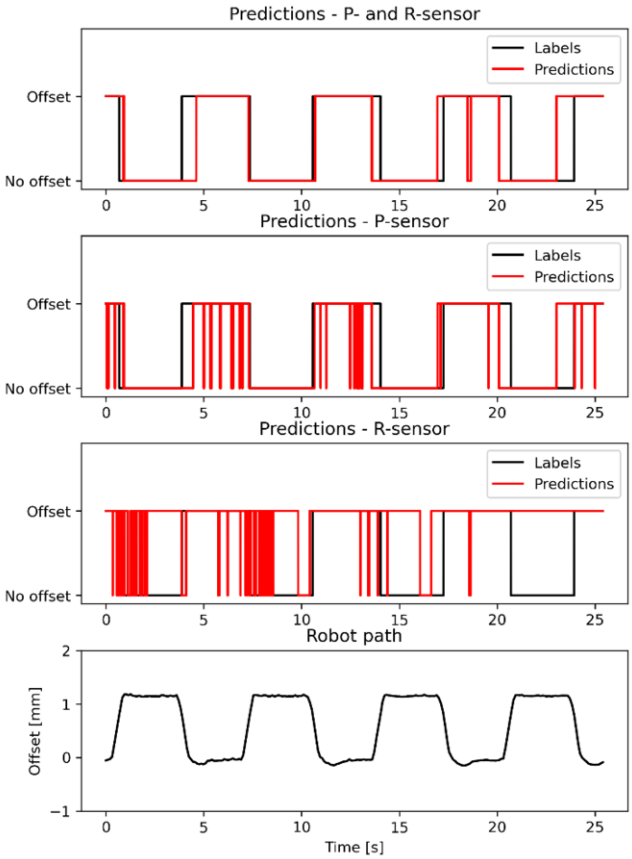

Figure 8. Prediction results from running three different models.

5. Conclusions

From the investigation conducted in this paper it can be concluded that

- There exists a clear correlation between the optical emissions from the LBW process, measured by the P- and R-sensor, and the beam offsets.
- Models trained by using One-class SVM gave an 86 % accuracy when using both the P- and R-sensor or only the P-sensor, and a 56 % accuracy when only using the R-sensor.

- Even though the model using both the P- and the R-sensor and the model using only the P-sensor gave the same accuracy, the model using both sensors gave less misclassifications when welding with an offset.
- It has been shown that training a model based on photodiode signals from a nominal test case can be useful to detect beam offsets during laser welding of closed square butt joints.

References

1. KG PG& C. WeldMaster 4.0 Track | high precision tracking | PRECITEC [Internet]. [cited 2023 Sep 19]. Available from: https://www.precitec.com/laser-welding/products/process-monitoring/weldmaster-track/

2. Eriksson I, Kaplan AF. Evaluation of laser weld monitoring A case study. In: Proceedings of ICALEO [Internet]. 2009 [cited 2014 Oct 17]. p. 1419–25. Available from: https://pure.ltu.se/portal/files/3347975/Laser_weld_monitoring.pdf

3. Eriksson I, Powell J, Kaplan AFH. Signal overlap in the monitoring of laser welding. Meas Sci Technol. 2010 Oct 1;21(10):105705.

4. Olsson R, Eriksson I, Powell J, Kaplan AFH. Advances in pulsed laser weld monitoring by the statistical analysis of reflected light. Optics and Lasers in Engineering. 2011 Nov;49(11):1352–9.

5. Kawahito Y, Ohnishi T, Katayama S. In-process monitoring and feedback control for stable production of full-penetration weld in continuous wave fibre laser welding. Journal of Physics D: Applied Physics. 2009 Apr 21;42(8):085501.

6. Sibillano T, Ancona A, Rizzi D, Lupo V, Tricarico L, Lugarà PM. Plasma Plume Oscillations Monitoring during Laser Welding of Stainless Steel by Discrete Wavelet Transform Application. Sensors. 2010 Apr 8;10(4):3549–61.

7. Elefante A, Nilsen M, Sikström F, Christiansson AK, Maggipinto T, Ancona A. Detecting beam offsets in laser welding of closed-square-butt joints by wavelet analysis of an optical process signal. Optics & Laser Technology. 2019 Jan 1;109:178–85.

8. Lee K, Kang S, Kang M, Yi S, Kim C. Estimation of Al/Cu laser weld penetration in photodiode signals using deep neural network classification. Journal of Laser Applications. 2021 Nov 1;33(4):042009.

9. Chianese G, Franciosa P, Sun T, Ceglarek D, Patalano S. Using photodiodes and supervised machine learning for automatic classification of weld defects in laser welding of thin foils copper-to-steel battery tabs. Journal of Laser Applications. 2022 Nov 1;34(4):042040.

10. Zhang Y, You D, Gao X, Zhang N, Gao PP. Welding defects detection based on deep learning with multiple optical sensors during disk laser welding of thick plates. Journal of Manufacturing Systems. 2019 Apr 1;51:87–94.

11. Schölkopf B, Williamson RC, Smola A, Shawe-Taylor J, Platt J. Support Vector Method for Novelty Detection. In: Solla S, Leen T, Müller K, editors. Advances in Neural Information Processing Systems [Internet]. MIT Press; 1999. Available from: https://proceedings.neurips.cc/paper_files/paper/1999/file/8725fb777f25776ffa9076e44fcfd776-Paper.pdf